Novel mm-Wave Oscillator Based on an Electromagnetic Bandgap Resonator

Enrico Lia, Indra Ghosh, Stephen M. Hanham, *Senior Member, IEEE*, Benjamin Walter, Fuanki Bavedila, Marc Faucher, Andrew P. Gregory, Leif Jensen, Jan Buchholz, Horst Fischer, Ulrich Altmann, and Rüdiger Follmann

***Abstract*— This letter introduces a novel millimeter (mm)-wave oscillator concept based on an electromagnetic bandgap (EBG) resonator (also called a photonic crystal resonator). To realize an ultralow phase noise monolithic microwave integrated circuit (MMIC) oscillator, an EBG resonator is developed by introducing a periodic structure into an ultrahigh resistivity silicon wafer to create an EBG which confines a localized resonant mode with a reduced mode dielectric filling factor of 47%. The measured results of the resonator demonstrate an unloaded Q-factor of 108300 can be achieved at 45 GHz. Measured oscillator phase noise levels of −91.5, −121.5, and −133 dBc/Hz are obtained at offset frequencies of 1, 10, and 100 kHz, respectively.**

***Index Terms*— Dielectric materials, dielectric resonator, microwave oscillators, monolithic microwave integrated circuits (MMICs), photonic crystals.**

I. Introduction

NOWADAYS, reference oscillators based on quartz resonators are limited in frequency of operation to a few hundred megahertz. Deriving gigahertz range signals from such a reference requires frequency multiplication or frequency synthesis. However, the multiplication process increases the phase noise of the output signal according to 20 $\log_{10}$ of the multiplication factor, as well as increasing the complexity of the circuit. In this sense, it is advantageous to have a local oscillator (LO) signal generated directly at the fundamental frequency in the millimeter (mm-) wave band. This requires, however, a high quality (Q-) factor resonator operating preferably at several gigahertz. Traditional passive resonators employing metal cavities have their Q-factor limited by the resistive losses in the metal. Alternatively, oscillators operating directly at the fundamental frequency based on ceramic resonators offer average phase noise and are normally not available above 25 GHz.

Dielectric resonators made of low dielectric loss and high resistivity materials are an interesting alternative to overcoming the problem of limited resonator Q-factors in the mm-wave band. One approach is to fabricate the dielectric resonator from an ultrahigh resistivity silicon wafer [1]. An emerging type of mm-wave dielectric resonator that can be implemented using a silicon wafer is an electromagnetic bandgap (EBG) resonator, also known as a photonic crystal resonator [2], [3]. Such a resonator is realized by engineering an EBG in the silicon wafer through the introduction of periodic holes in order to confine a localized resonant mode. A resonator designed in this manner may have a Q-factor limited only by material loss. This material loss may be reduced by designing the resonator in such a way as to concentrate most of the energy outside the silicon and in air. This approach allows the realization of extremely high Q-factors which is a key aspect to achieving very low phase noise in oscillator applications.

Research papers and laboratory demonstrations [4], [5] have shown that dielectric resonators made from low-loss materials such as high-resistivity silicon may become an interesting alternative to conventional room-temperature passive mm-wave resonators used in reference and high-frequency oscillators, and important components for future mm-wave applications.

This work aims to demonstrate that low-loss ultrahigh resistivity silicon resonators can be utilized for high-frequency oscillators with significant advantages in obtaining high Q-factor and therefore low phase noise compared to multiplied quartz crystals and traditional high-frequency oscillators. In this letter, the novel experiment of using a silicon EBG resonator exhibiting a reduced dielectric filling factor of its resonant mode in an oscillator operating at 45 GHz is demonstrated successfully, establishing a route toward overcoming the problem of excessive phase noise affecting high-frequency oscillators operating in the mm-wave band.

II. Ultrahigh Q-Factor Resonator Design

Low-loss and high-performance dielectric materials are crucial for realizing dielectric resonators as part of oscillators in high-performance telecommunication systems. The dielectric material chosen for the investigation and characterization of

Manuscript received 7 March 2023; revised 11 April 2023 and 13 April 2023; accepted 14 April 2023. This work was supported in part by the European Space Agency under Contract 4000130082/20/NL/HK and in part by the U.K. Engineering and Physical Sciences Research Council (EPSRC) under Contract EP/V001655/1. *(Corresponding author: Enrico Lia.)*

Enrico Lia is with the European Space Agency, ESA-ESTEC, 2200AG Noordwijk, The Netherlands (e-mail: enrico.lia@ext.esa.int).

Indra Ghosh, Jan Buchholz, Horst Fischer, Ulrich Altmann, and Rüdiger Follmann are with IMST GmbH, 47475 Kamp-Lintfort, Germany (e-mail: indra.ghosh@imst.de; jan.buchholz@imst.de; horst.fischer@imst.de; ulrich.altmann@imst.de; ruediger.follmann@imst.de).

Stephen M. Hanham is with the Department of Electronic, Electrical and Systems Engineering, University of Birmingham, B15 2TT Birmingham, U.K. (e-mail: s.hanham@bham.ac.uk).

Benjamin Walter and Fuanki Bavedila are with Vmicro SAS, 59650 Villeneuve-d'Ascq, France (e-mail: benjamin.walter@vmicro.fr; fuanki.bavedila@vmicro.fr).

Marc Faucher is with Vmicro SAS, 59650 Villeneuve-d'Ascq, France, and also with the University of Lille, CNRS, Centrale Lille, University Polytechnique Hauts-de-France, UMR 8520 - IEMN - Institut d'Electronique de Microélectronique et de Nanotechnologie, F-59000 Lille, France (e-mail: marc.faucher@vmicro.fr).

Andrew P. Gregory is with the National Physical Laboratory, TW11 0LW Middlesex, U.K. (e-mail: andrew.gregory@npl.co.uk).

Leif Jensen is with Topsil GlobalWafers A/S, 3600 Frederikssund, Denmark (e-mail: lej@gw-topsil.com).

This article was presented at the IEEE MTT-S International Microwave Symposium (IMS 2023), San Diego, CA, USA, June 11–16, 2023.

Color versions of one or more figures in this letter are available at https://doi.org/10.1109/LMWT.2023.3268090.

Digital Object Identifier 10.1109/LMWT.2023.3268090

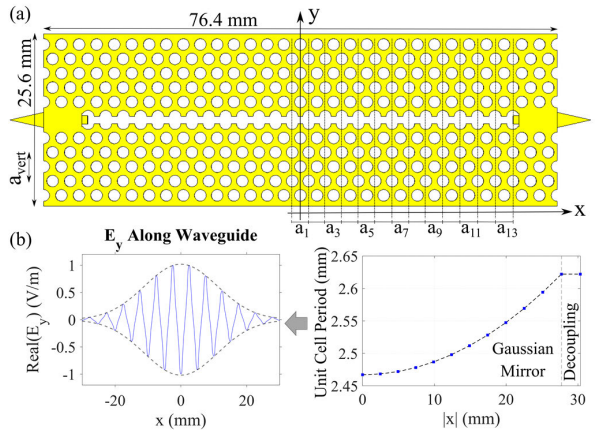

Fig. 1. (a) EBG resonator with its dimensions and variable periodicity (a_n) along the x-axis. (b) Gaussian envelope of the resonant mode achieved by linearly increasing the reflection from the center to the outer unit cells.

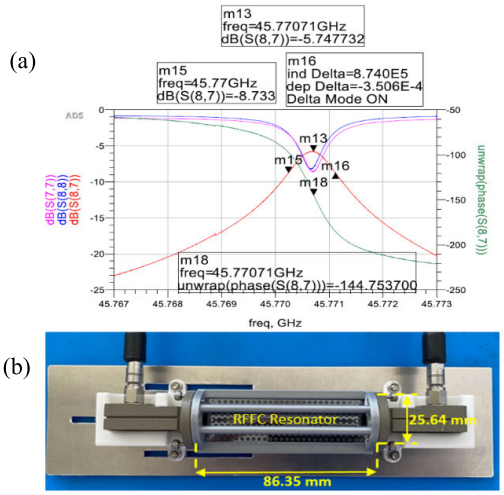

Fig. 2. (a) Measured results of the two-port S-parameters (amplitude and unwrapped phase of the forward transmission $S_{8,7}$, and input reflection $S_{7,7}$ and $S_{8,8}$ amplitudes) coefficients. (b) EBG resonator in its test jig interfaced with the waveguide-to-coaxial adapters.

the resonator is the high-resistivity silicon for GHz and THz applications supplied by Topsil GlobalWafers A/S [4].

The design of the silicon EBG resonator relies upon the creation of a surrounding region of the silicon exhibiting an EBG and this is realized using a triangular lattice of air holes perforating the planar silicon wafer. The resulting transverse electric (TE)-like bandgap is defined according to the substrate parameters (e.g., its height as well as the hole diameter and the lattice constant). The neutron-irradiated (NTD) high-resistivity silicon (HRS) used has a measured permittivity ε_r equal to 11.68 and loss tangent $\tan\delta$ of 1.2×10^{-5} (294 K), including both dielectric and finite conductivity losses. The substrate has a thickness of 1000 μm, the holes have a radius of 863.5 μm, and a lattice constant of 2467 μm. The periodic EBG structure prohibits propagating modes within its bandgap and the energy stored inside a localized mode cannot be transported through this region of the silicon wafer.

The resonator is formed by the concatenation of unit cells with a small increase in horizontal width period from the central unit cell to the outer unit cells, as shown in Fig. 1, to confine the resonant mode. The unit cell analysis is performed assuming infinite periodicity in the x-axis directions. The unit cells are engineered so that the majority of the propagating mode's energy is concentrated in an air gap rather than silicon. The approach introduced here employs the idea of reducing the dielectric filling factor of the resonator to reduce overall dielectric loss of the resonator. The filling factor κ is defined as the ratio of the electromagnetic energy of a resonator stored inside the silicon to the total stored electromagnetic energy. By lowering κ, the achievable quality factor increases according to $1/(\kappa \tan\delta)$, with $\tan\delta$ being the loss tangent of the silicon substrate material.

The filling factor can be expressed as follows:

$$\kappa = \frac{\iiint_{V_{si}} \epsilon_{si}|E|^2 dv}{\iiint_{V_t} \epsilon(v)|E|^2 dv} \tag{1}$$

where V_{si} is the volume of the silicon forming the EBG resonator and V_t is the total volume containing the resonant mode. The denominator represents the total energy of the mode. To minimize out-of-plane losses, it is necessary to shape the electric and magnetic field in the resonator to reduce wave-vector components inside the light cone [6], [7]. A common approach is to create a Gaussian envelope of the field by linearly increasing reflection from the center to outer unit cells. This is achieved by varying the horizontal period (width) of the unit cells quadratically with the distance in the $\pm x$-directions, as shown in Fig. 1.

The EBG resonator design has been simulated using a range of tools implementing different techniques such as Meep with FDTD (time-domain) and rectangular grid meshing, Computer Simulation Technology (CST) Microwave Studio with finite element method (FEM) and tetrahedral meshing, and Empire XPU tool. After careful optimization of the parameters and best simulation results obtained, the EBG resonator was manufactured. An NTD float zone silicon wafer with high resistivity (>4 00 000 Ω·cm), 150-mm diameter, and 1000-μm thickness is etched using the deep reactive-ion etching (DRIE) method, which is a highly anisotropic process to achieve deep etch depths with steep-sided holes and trenches in wafer substrates.

The measurement results of the full two-port S-parameters achieved an outstanding loaded Q-factor (Q_L) of 52 400 with insertion loss peak $S_{8,7}$ of −5.75 dB, shown in Fig. 2. The unloaded Q-factor (Q_u) is calculated to be 1 08 300 at 45.77 GHz using $Q_u = Q_L/(1 - |S_{8,7}(f_0)|)$, where Q_L is calculated from the forward transmission $S_{8,7}$ using the 3-dB method and f_0 is the resonant frequency. It is important to highlight the importance of obtaining an insertion loss of approximately –6 dB to achieve the best phase noise results in oscillator applications [8], [9].

III. Voltage-Controlled Oscillator (VCO) Monolithic Microwave Integrated Circuit (MMIC) Design

The design approach of the active circuit is based on a monolithic microwave integrated circuit (MMIC) voltage-controlled oscillator (VCO) using a high-performance 130-nm SiGe BiCMOS semiconductor technology process from Innovations for High Performance (IHP) Microelectronics with a cutoff frequency F_T up to 250 GHz and a maximum frequency $F_{\text{max}} = 340$ GHz. The oscillator has been realized in feedback topology: the MMIC contains a two-stage loop amplifier (black and red regions in Fig. 3) whose second stage has been designed in a balanced configuration, a 10-dB coupler (yellow) which serves to supply the oscillator signal to the output. This is followed by an electronic phase shifter realized by a 90° hybrid coupler (blue) which is terminated by varactor diodes at two ports. The total gain realized within

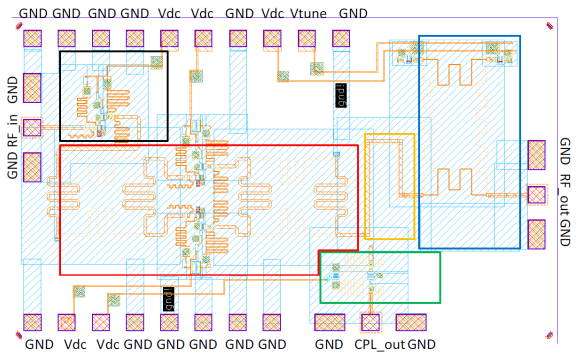

Fig. 3. Layout of the MMIC VCO circuit.

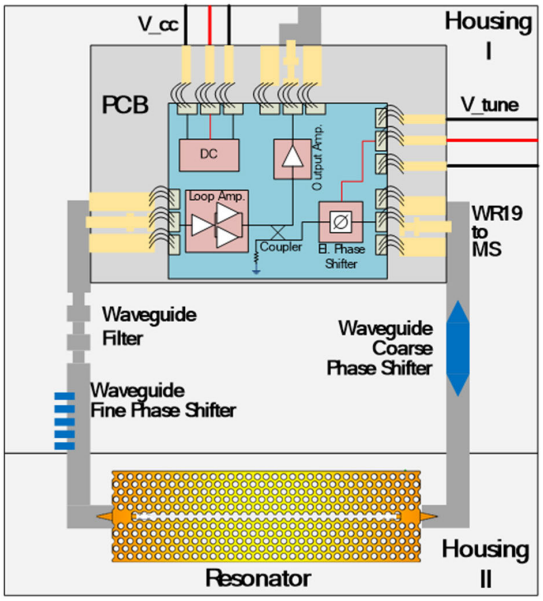

Fig. 4. Complete block diagram of the MMIC VCO.

the oscillator loop is 12.5 dB. To couple to the TE_{10} mode in the feed waveguides, the input and output of the circuit are connected through bond-wires to waveguide (WR-19) to microstrip transition probes. The waveguides include a waveguide bandpass filter and fine and coarse phase-shifters and connect to the EBG resonator through triangular tapers created on the edge of the silicon substrate which protrude inside a standard WR-19 waveguide to couple to the TE_{10} mode. The output of the RF signal is obtained after an output amplifier (green region in Fig. 3) with a gain of 7.8 dB connected in the same way to a waveguide to coaxial adapter.

IHP Microelectronics provides an SG13S design kit for the advanced design systems (ADS) simulation tool used in the design of the oscillator.

Fig. 4 shows the block diagram for the MMIC oscillator and Fig. 5 shows the assembled oscillator inside its housing. The total power consumption of the oscillator is 215 mW, size is 157 × 88 × 29 mm, and the weight is 442 g, including all connectors.

The loss tangent of silicon has a sharp increase for temperatures higher than 290 K [10]. To avoid this region, a nominal operation temperature for the oscillator of 263 K is chosen as a compromise between increased cooling power requirements and higher Q-factor. Fig. 6 shows the measured phase noise levels of −94.6, −120.3, and −142.6 dBc/Hz obtained at offset frequencies of 1, 10, and 100 kHz, respectively, with an output power of −1.2 dBm at a nominal impedance of 50 Ω at 263 K with zero tuning voltage. The oscillator also works at room temperature (290 K) with a corresponding degradation of 2–6 dB in terms of single sideband (SSB) phase noise.

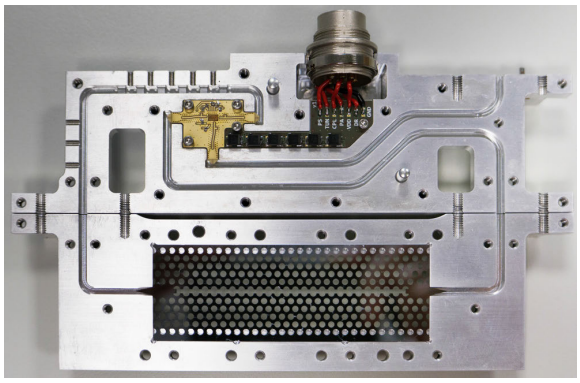

Fig. 5. Final MMIC VCO assembly in its housing (top half removed).

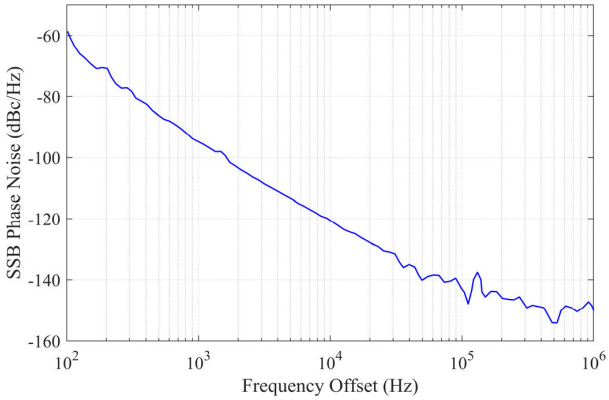

Fig. 6. Measured SSB phase noise of the oscillator at 263 K.

TABLE I

COMPARISON OF STATE-OF-THE-ART MICROWAVE AND MM-WAVE OSCILLATORS. ALL SSB PHASE NOISE VALUES WERE NORMALIZED TO A 45-GHZ CARRIER FREQUENCY AND ESTIMATED VALUES, SHOWN IN GRAY, WERE ESTIMATED BASED ON THE INTERCEPT WITHIN THE SLOPE REGIONS

Ref.	Description	Pout [dBm]	SSB PN [dBc/Hz] @ offset	FOM [dBc/Hz]
[11]	Tunable DRO @ 12.8 GHz	+17.0	-33 @ [100 Hz] -65 @ [1 KHz] -96 @ [10 KHz] -122 @ [100 KHz -141 @ 1MHz -150 @ 10 MHz	156
[12]	0.18 um CMOS Quadrature VCO (20 GHz)	-6.8	-5 @ [100 Hz] -12 @ [1 KHz] -42 @ [10 KHz] -72 @ [100 KHz] -105 @ [1MHz] -114 @ [10 MHz]	181.5
[13]	Quad. SiGe HBT MMIC VCO (38.5 GHz)	-7.5	-11@ 100 Hz -41 @ 1 KHz] -49 @ [10 KHz] -61 @ [100 KHz] -73 @ [1MHz] -84 @ [10 MHz]	151
[14]	WGM-based Optoelectronic Oscillator (11 GHz)	-15.0	-19 @ [100 Hz] -51 @ [1 KHz] -79 @ [10 KHz] -106 @ [100 KHz] -135 @ [1MHz] -143 @ [10 MHz]	-
This work	EBG Oscillator (45.8 GHz)	-1.7	-57 @ [100 Hz] -95 @ [1 KHz] -120 @ [10 KHz] -142 @ [100 KHz] -151 @ [1MHz] -153 @ [10 MHz]	230

Owing to the temperature variation of the silicon permittivity and the reduced dielectric filling factor of the resonator of 47%, the temperature drift of the oscillator frequency is 1 MHz/K. By means of PID temperature control and thermally isolating the oscillator from the environment, it is expected that a temperature stability of $<\pm 0.05$ K can be achieved resulting in a remaining frequency variation of ± 50 kHz. The electrical tuning range of the oscillator is 239 kHz (0–3 V), which is limited by the operation of the phase shifters within the narrow passband of the resonator. Further precise frequency adjustment can be carried out by means of the tuning voltage or varying the resonator temperature.

Table I compares the overall performance of the oscillator with other microwave and mm-wave oscillators described in the literature. It can be seen that the oscillator compares favorably in terms of phase noise and figure of merit (FOM) performance with state-of-the-art oscillators. The oscillator FOM is defined as $\mathrm{FOM} = L(\Delta f) - 20\log(f_0/\Delta f) + 10\log(P_{DC}/1\,\mathrm{mW})$, where $L(\Delta f)$ is the phase noise in dBc/Hz at the frequency offset Δf from the oscillator frequency f_0, and P_{DC} is the total power consumption.

IV. Conclusion

This letter demonstrates a novel mm-wave oscillator employing a low-loss HRS resonator with a reduced dielectric filling factor of its resonant mode, leading to an improved Q-factor, thereby addressing the problem of excessive phase noise affecting high-frequency oscillators operating in the mm-waveband. The oscillator also benefits from small size and low power consumption. Future work is to increase the technology readiness level (TRL) of the oscillator, improve the frequency stability and tunability, and realize scaled versions operating at higher fundamental mode frequencies.

Acknowledgment

For the purpose of open access, the author(s) has applied a Creative Commons Attribution (CC BY) license to any Accepted Manuscript version arising.

References

[1] J. Krupka, P. Kaminski, and L. Jensen, "High Q-factor millimeter-wave silicon resonators," *IEEE Trans. Microw. Theory Techn.*, vol. 64, no. 12, pp. 4149–4154, Dec. 2016.

[2] J. D. Joannopoulos, S. G. Johnson, J. N. Winn, and R. D. Meade, *Photonic Crystals: Molding the Flow of Light*, 2nd ed. Princeton, NJ, USA: Princeton Univ., 2011.

[3] W. J. Otter, S. M. Hanham, N. M. Ridler, G. Marino, N. Klein, and S. Lucyszyn, "100 GHz ultra-high Q-factor photonic crystal resonators," *Sens. Actuators A, Phys.*, vol. 217, pp. 151–159, Sep. 2014.

[4] L. Jensen, "High resistivity (HiResTM) silicon for GHz & THz technology," Topsil Company, Denmark, U.K., Tech. Rep., v1.1, Jan. 2014.

[5] J. Krupka, J. Breeze, N. A. Centeno, and N. Alford, "Measurements of permittivity and dielectric loss tangent of high resistivity float zone silicon at microwave frequencies," *IEEE Trans. Microw. Theory Techn.*, vol. 54, no. 11, pp. 3995–4001, Nov. 2006.

[6] Y. Tanaka, T. Asano, and S. Noda, "Design of photonic crystal nanocavity with Q-factor ~10^9," *J. Lightw. Technol.*, vol. 26, no. 11, pp. 1532–1539, Jun. 15, 2008.

[7] Y. Akahane, T. Asano, B.-S. Song, and S. Noda, "High-Q photonic nanocavity in a two-dimensional photonic crystal," *Nature*, vol. 425, pp. 944–947, Oct. 2003.

[8] J. K. A. Everard, "Low noise oscillators," in *IEEE MTT-S Int. Microw. Symp. Dig.*, Albuquerque, NM, USA, Jun. 1992, pp. 1077–1080.

[9] E. Lia, R. Dionisio, M. Kucharski, M. A. G. Lasso, A. Gómes-Torrent, and I. Arregui, "High Q-factor silicon resonator for high frequency oscillators," in *Proc. Microw. Technol. Techn. Workshop*, Apr. 2017.

[10] J. Krupka, W. Karcz, P. Kamiński, and L. Jensen, "Electrical properties of as-grown and proton-irradiated high purity silicon," *Nucl. Instrum. Methods Phys. Res. B, Beam Interact. Mater. At.*, vol. 380, pp. 76–83, Aug. 2016.

[11] R. Kaesbach, M. Van Delden, and T. Musch, "A fixed-frequency, tunable dielectric resonator oscillator with phase-locked loop stabilization," in *Proc. Asia–Pacific Microw. Conf. (APMC)*, Yokohama, Japan, Nov. 2022, pp. 728–730.

[12] S. Koo, J.-G. Kim, T. Song, E. Yoon, and S. Hong, "20 GHz integrated CMOS frequency sources with a quadrature VCO using transformers," in *IEE Radio Freq. Integr. Circuits (RFIC) Syst., Dig. Papers*, Forth Worth, TX, USA, Jun. 2004, pp. 269–272.

[13] A. Dyskin, S. Wagner, and I. Kallfass, "A compact resistive quadrature low noise Ka-band VCO SiGe HBT MMIC," in *Proc. 12th German Microw. Conf. (GeMiC)*, Stuttgart, Germany, Mar. 2019, pp. 95–98.

[14] D. Eliyahu et al., "Ultra-wideband photonic VCO and synthesizer," in *IEEE MTT-S Int. Microw. Symp. Dig.*, Atlanta, GA, USA, Jun. 2021, pp. 538–540.